Future projections of daily haze conducive and clear weather conditions over the North China Plain using a Perturbed Parameter Ensemble

Shipra Jain[1,2], Ruth M. Doherty[1], David Sexton[3], Steven Turnock[3,4], Chaofan Li[5], Zixuan Jia[1], Zongbo Shi[6], Lin Pei[7]

[1]School of GeoSciences, The University of Edinburgh, Edinburgh, United Kingdom

[2]Centre for Climate Research Singapore (CCRS), Singapore

[3]Met Office Hadley Centre, Exeter, United Kingdom

[4]University of Leeds Met Office Strategic (LUMOS) Research Group, School of Earth and Environment, University of Leeds, UK

[5]Center for Monsoon System Research, Institute of Atmospheric Physics, Chinese Academy of Sciences, China

[6]School of Geography, Earth and Environmental Sciences, University of Birmingham, Birmingham, United Kingdom

[7]Institute of Urban Meteorology, China Meteorological Administration, Beijing, China

Corresponding Author: Shipra Jain (Shipra.Jain@ed.ac.uk)

Abstract

We examine past and future changes in both winter haze and clear weather conditions over the North China Plain (NCP) using a Perturbed Parameter Ensemble (PPE) and elucidate the influence of model physical parameterizations on these future projections for the first time. We use a large-scale meteorology-based Haze Weather Index (HWI) with values >1 as a proxy for haze conducive weather and HWI <-1 for clear weather conditions over the NCP. The PPE generated using the UK Met Office HadGEM-GC3 model shows that under a high-emission (RCP8.5) scenario, the frequency of haze conducive weather (HWI>1) is likely to increase whereas the frequency of clear weather (HWI<-1) is likely to decrease in future, with a growing influence of climate change over the 21st century. Nevertheless, a change of opposite sign with lower magnitude in the frequencies, though less likely, is also possible. In future, the frequency of haze conducive weather for a given winter can be as much as ~3.5 times higher than the frequency of clear weather over the NCP. More frequent haze conducive weather (HWI>1) during winter over the NCP is found to be associated with an enhanced warming of the troposphere and weaker north-westerlies in the mid-troposphere over the NCP. We also examined the changes in the interannual variability of the haze conducive and clear weather and find no marked changes in the variability of future periods. We find a clear influence of model physical parametrizations on climatological mean frequencies for both haze conducive and clear weather. For mid to late 21st century (2033-2086), parametric effect can explain up to ~80% variance in climatological mean frequencies of PPE members. This shows that the different model physical parameterizations lead to a different evolution of model's mean climate, particularly towards the end of the 21st century. Therefore, it is desirable to consider the PPE in addition to the initialized and multimodel ensembles for a more comprehensive range of plausible future projections.

1. Introduction

Over the last decade, a number of severe haze episodes (several days or longer) were reported over the North China Plain (NCP) during boreal winter (December-January-February, DJF). In January 2013, unprecedented $PM_{2.5}$ levels exceeding 450 μg m^{-3} were observed over the NCP (Wang et al., 2014a; Wang et al., 2014b; Zhang et al., 2018; Zhang et al., 2013). Similar events were also observed in November-December 2015 when the $PM_{2.5}$ concentrations reached as high as 1000 μg m^{-3} in Beijing and caused the first-ever 'red alert' for severe air pollution (Liu et al., 2017; Zhang et al., 2017). In December 2016, around 25% of the land area of China was covered with severe haze for around one week (Yin and Wang, 2017). These severe haze events adversely impacted public health including mortality, visibility, and ultimately the economy of the country (Bai et al., 2007; Chen and Wang, 2015; Kan et al., 2012; Kan et al., 2007; Wang et al., 2006; Xu et al., 2013; Hong et al., 2019).

Previous research has shown that the persistence of severe haze for days during winters over the NCP occurred due to the combined effect of local and regional high pollutant emissions and stagnant meteorological conditions (Li et al., 2018; He et al., 2016; Jia et al., 2015; Pei et al., 2018; Zhang et al., 2021). The normal winter meteorological conditions over the NCP are characterized by northwesterly flow near the surface through to the mid-troposphere associated with the East Asian winter monsoon circulation (Fig. 1a and 1b; also see An et al., 2019; Chen and Wang, 2015; Li et al., 2016; Renhe et al., 2014; Xu et al., 2006). The northwesterly winds support the intrusion of relatively clean air from the high latitudes to the NCP and therefore ventilate this region (Xu et al., 2006). However, during the severe haze episodes, the lower tropospheric (~850 hPa) northwesterlies appear to be weaker than normal and the mid-tropospheric trough was reported to be shallower and shifted northwards – collectively leading to a weaker than normal northwesterly flow and reduced horizontal transport of air pollutants from the NCP (Fig. 2a-b). In addition to changes in horizontal winds, the vertical temperature gradient between the lower and upper troposphere over the NCP can influence the vertical dispersion of the pollutants. A warmer than normal temperature in the lower troposphere (~850 hPa), accompanied with colder temperature in the upper troposphere (~200 hPa), would enhance the thermal stability and reduce the atmospheric mixing leading to the build-up of the atmospheric pollutants over this region (Fig. 2; also see Hou and Wu, 2016; Sun et al., 2014; Wang et al., 2014a; Zhang et al., 2018; Cai et al., 2018). The planetary boundary layer height is also found to be suppressed during extreme haze events leading to accumulation of pollutants, notably $PM_{2.5}$ concentrations (Liu et al., 2018; Petäjä et al., 2016), due to an increase in moisture, reduced vertical mixing and dispersion which aids aerosol growth during high haze events over the NCP (An et al., 2019; Tie et al., 2017).

On a daily scale, past studies have examined the changes in haze conducive weather conditions over China under climate change scenarios using large-scale meteorology-based indexes. For example, Cai et al. (2017) have used four key variables, i.e. meridional wind at 850 hPa (V_{850}), zonal wind at 500 hPa (U_{500}), temperatures at 850 hPa (T_{850}) and 250 hPa (T_{250}) pressure levels to calculate a meteorology-based daily Haze Weather Index (HWI). They have projected a ~50% increase in the frequency of winter haze conducive weather conditions, similar to the January 2013 event, over Beijing in the future (2050-2099) as compared to the historical (1950-1999) period under the RCP8.5 scenario using 15 CMIP5 models. Using the HWI, Liu et al. (2019) projected a 6-9% increase in the winter haze frequency under 1.5° and 2° global warming, respectively based on 20 CMIP5 models whereas Qiu et al. (2020) projected a relatively high increase of 21% and 18% in severe winter haze episodes under 1.5° and 2° global warming, respectively using an ensemble of climate simulations from the Community Earth System Model 1 (CESM1) (Kay et al., 2015). Callahan and Mankin (2020) also used specific humidity, V_{850}, T_{850} and temperatures at 1000 hPa to examine the haze favourable meteorology for Beijing, and found a 10-15% increase in winter haze conducive weather in CMIP5 multimodel and CESM large ensemble under 3° warming. These authors have also emphasized a large influence of internal variability in addition to anthropogenic forcing on future haze conducive weather over Beijing.

In addition to the large-scale meteorology based indexes, several other stagnation indices based on regional or local meteorological variables have also been used to determine the influence of anthropogenic climate change on haze conducive weather for China as well as global regions. Using minimum monthly mean wind speeds averaged over northwestern Europe, Vautard et al. (2018) suggested a potential increase in the frequency of stagnant conditions conducive to air pollution over northwest Europe; however, their results were sensitive to models used for the analysis. Horton et al. (2014) have used thresholds for the daily mean near-surface (10-m) wind speeds, mid-tropospheric (500 hPa) temperatures and accumulated precipitation to calculate the Air Stagnation Index (ASI) under RCP8.5 scenario using 15 CMIP5 models. They found an increase in air stagnation occurrence events leading to poor air quality by up to ~40 days per year over a majority of the tropics and sub-tropics. Han et al. (2017) examined indicators of haze pollution potential (e.g. horizontal transport, wet-deposition, ventilation conditions) using three regional climate simulations and projected a higher probability of haze pollution risk over the Beijing-Tianjin-Hebei region under the RCP4.5 scenario. Garrido-Perez et al. (2021) took a different approach as compared to analysing probabilistic projections and used the ASI to generate stagnation storylines, i.e. plausible and physically consistent scenarios of stagnation changes based on the response of remote drivers under climate change forcing, for Europe and the United States (US).

While most studies indicate an increase in the haze conducive weather over China, a few studies also find little impact of climate change on future projections of haze (Shen et al., 2018; Pendergrass et al., 2019), which could partly arise due to the under-sampling of internal variability associated uncertainty in their projections (Callahan and Mankin, 2020), as well as model-to-model differences. Hence, there is a large uncertainty as to how haze conducive weather conditions may change in the future and these depend on haze metrics or underlying processes considered for future projections.

In order to account for the uncertainty in the future projections (e.g. of large-scale circulation) particularly at the regional scale (Hawkins and Sutton, 2012; Deser et al., 2012; Deser et al., 2014), it is desirable to use an ensemble of climate change simulations. Whilst a multimodel ensemble, e.g. CMIP5 or CMIP6, is commonly used for climate change studies, several other studies have also emphasised the use of an initialised ensemble or Perturbed Parameter Ensemble (PPE) from a single model to assess the uncertainties and obtain a comprehensive range of possible future climate realisations for the same emission scenario for a given model (Knutti et al., 2010). All three methodologies have different advantages. For instance, using multiple models allows us to sample structural uncertainty in future projections, which cannot be sampled using a single model. On the other hand, using an initialised ensemble from a single model allows us to sample a broader range of internal variability, which is often under-sampled in a multimodel ensemble. The advantage of using the PPE over the initialised or multimodel ensemble is that it not only accounts for internal variability but also model uncertainty arising due to the different settings of the physical parameterisations in a single model. Both multimodel ensemble and initialised ensemble from a single model have been used to assess the future winter haze conducive conditions over Beijing. In this paper, we use a PPE generated using the UK's Met Office HadGEM-GC3 model to assess for the first time the impact of both model physical parameterisations and anthropogenic climate change on future daily haze conducive weather conditions.

In this paper, our focus is on the daily haze conducive and clear weather conditions over the NCP under a fixed high-emission scenario (RCP8.5). For this purpose, we use the HWI proposed by Cai et al. (2018) as past research studies have shown a robust correlation between the HWI, which is a large-scale meteorology based index, and haze conducive weather for Beijing in China. Whilst Cai et al. (2018) originally proposed the HWI for Beijing, the index is based on changes in large-scale meteorology over the NCP and thus offers a good potential as the indicator of haze conducive weather over the NCP. One potential advantage of using the HWI for future projections, as opposed to a regional or local air stagnation index, is that the general circulation models generally simulate large-scale meteorology reasonably well as compared to local or regional meteorology. Therefore, we expect the future projections of clear or haze conducive weather provided using the HWI to be less uncertain than projections provided using regional stagnation indexes.

The HWI uses four meteorological variables as stated above, but Cai et al. (2018) have also examined the impact of the inclusion of more weather variables, such as geopotential height, boundary layer thickness and local stratification instability, in the HWI and did not find any significant differences in the performance of the HWI. Therefore, we use the same variables and methodology as Cai et al (2018) to calculate the HWI and provide future projections of haze conducive and clear weather using the HWI. However, our analysis is based on an underlying assumption that the large-scale meteorological conditions, which are used as a basis for the HWI, will have a similar influence on the air quality of the NCP in the future climate as for present-day climate.

In this paper, we first examine the application of the HWI as a proxy for haze conducive and clear weather over NCP for the current climate using a suite of observations (Section 3). We then provide the projections of the haze conducive (HWI >1) and clear weather (HWI <-1) frequency over NCP for the historical and future period. We assess the impact of model physical parametrisations and anthropogenic climate change on the frequencies (Section 4). We also analyse the changes in the interannual variance of the frequency of haze conducive and clear weather conditions for the future periods as compared to the historical period (Section 5). Finally, we assess the impact of parametric effect and anthropogenic climate change on trends in haze conducive and clear weather occurrence over the 21st century (Section 6). Details of data and methods used in this paper are provided in the next section.

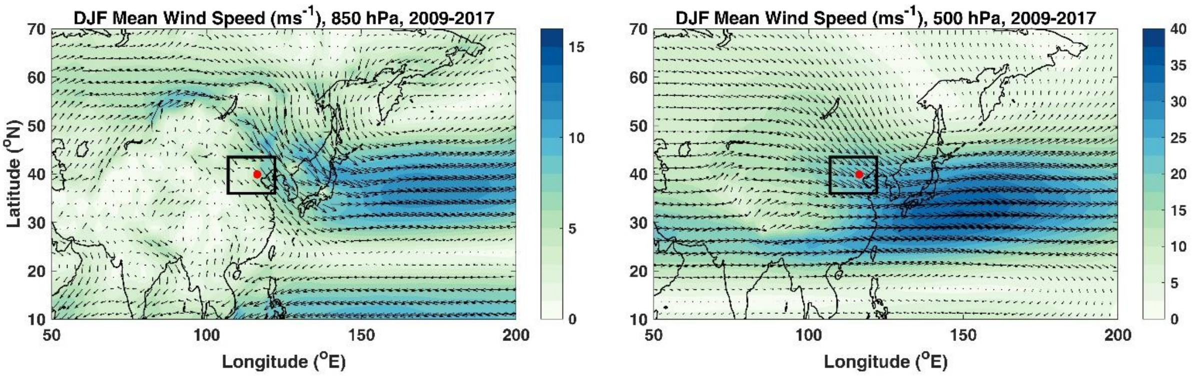

Figure 1 Average wind speed at (a) 850 hPa and (b) 500 hPa pressure level. The red dot represents the location of Beijing and black rectangle shows the location of the NCP. This figure has been repeated for a longer average period, i.e. 1979-2019 (not shown) and the result is similar.

2. Data & Methods

2.1 Observations, Reanalysis Outputs and PPE Model Simulations

Hourly $PM_{2.5}$ concentrations are used from the US embassy site for Beijing for DJF from 2009-2017. Daily mean $PM_{2.5}$ concentrations are constructed using hourly data to evaluate the performance of the HWI as a representative of haze conducive and clear weather conditions for Beijing (see Section 3). We also used newly released gridded daily $PM_{2.5}$ concentrations for DJF from Chinese Air Quality Reanalysis Datasets (CAQRA) provided by China National Environment Monitoring Centre for 2013-2017 (Kong et al., 2021) to test the performance of the HWI across entire China. The CAQRA data has been produced by assimilating surface air quality observations from over 1000 monitoring sites in China and is available at a high spatial resolution of around 15×15 km and hourly temporal resolution over China. More details on the validation of the CAQRA dataset against the independent station data is provided in Kong et al. (2021). The visibility data for Beijing (homogenized data for 20 stations in Beijing) is provided by the National Meteorological Information Center of China, China Meteorological Administration (CMA), for DJF 1999-2018.

We used daily ERA-5 reanalysis data of four variables: meridional wind at 850 hPa pressure level (V_{850}), zonal wind at 500 hPa pressure level (U_{500}), temperatures at 850 hPa level (T_{850}) and 250 hPa (T_{250}) to calculate the HWI for DJF 1979-2019. The ERA-5 data used here is available at 0.25° x 0.25° horizontal resolution and hourly temporal resolution (Hersbach et al., 2020).

We used a PPE of climate simulations produced using the recent configuration of the UK Met Office's HadGEM3-GC3.05 coupled model (Sexton et al., 2021; Yamazaki et al., 2021). The base model used for PPE, HadGEM3-GC3.05, has a horizontal resolution of ~60 km with 85 vertical levels. A total of 47 model parameters from seven parameterization schemes were simultaneously perturbed to obtain the PPE (the full list of perturbed parameters is provided in Table 1 of (Sexton et al., 2021). Here, we used daily outputs of V_{850}, U_{500}, T_{850} and T_{250} for DJF for the historical (1969-2005) and future (2006-2089) under the RCP8.5 scenario. In addition, we also assessed internal variability using 200-year control simulations for each PPE member where 1900 boundary conditions were prescribed. Overall, 16 PPE members are available for all the control, historical and RCP8.5 simulations

2.2 Calculation of the HWI

The winter HWI is calculated using the methodology given by Cai et al. (2017). We analyse the composite differences in the U_{500}, V_{850}, T_{850} and T_{250} for hazy ($PM_{2.5}$ concentrations > 150 μg m^{-3} for Beijing) and clear ($PM_{2.5}$ concentrations < 35 μg m^{-3} for Beijing) days across China for DJF 2009-2017 (Fig. 2) (see section 3.1 for an explanation on the $PM_{2.5}$ concentration cut-offs values used here). We also provide the composite values for these meteorological variables for hazy and clear days separately in Fig. 2.

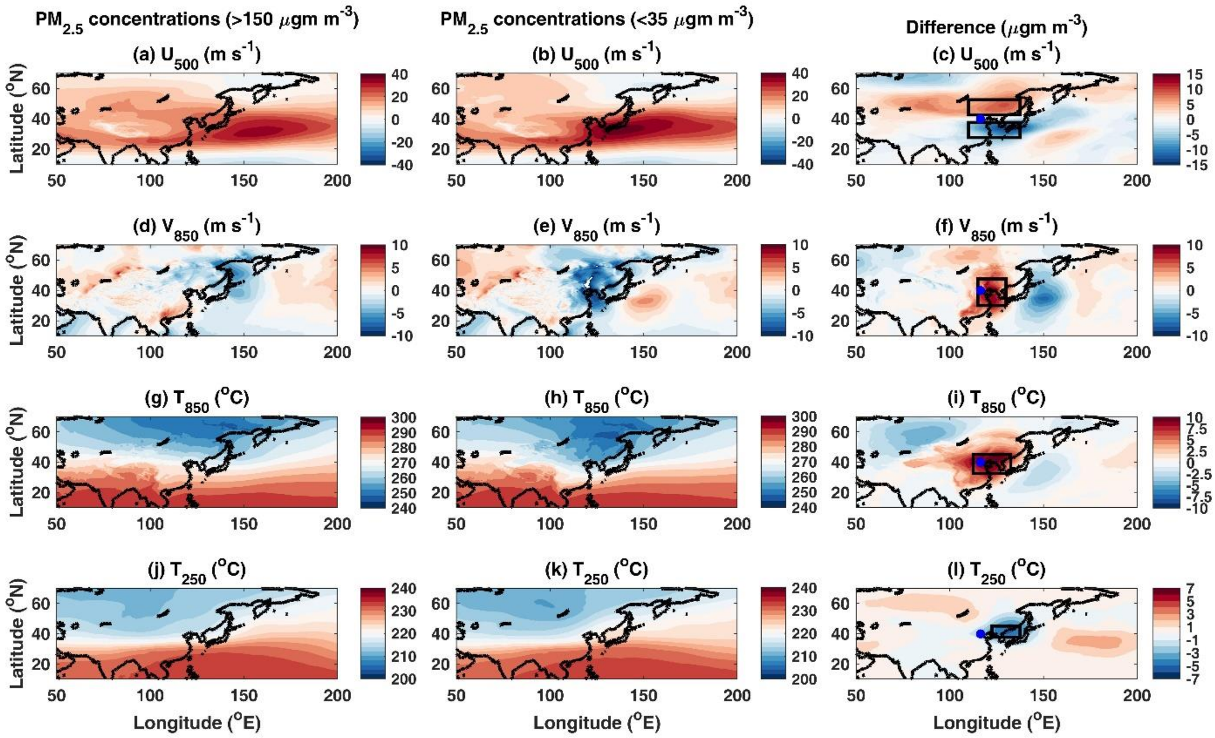

Figure 2 Winter composites of u-wind at 500 hPa level (U_{500}) over China for all available days for which data is available from US embassy station for Beijing for DJF 2009-2017 for **(a)** high $PM_{2.5}$ (>150 μgm m^{-3}), **(b)** low $PM_{2.5}$ (<35 μgm m^{-3}) concentrations and **(c)** difference between the composites in (a) and (b). **(d-f)** same as (a-c) but for v-wind at 850 hPa level (V_{850}), **(g-i)** same as (a-c) but for temperature at 850 hPa level (T_{850}), and **(j-l)** same as (a-c) but for temperature at 250 hPa pressure level (T_{250}). Black rectangles (B1-B5) in the last column show the regions for which spatial means were used for the calculation of the HWI. The blue dot in these columns shows the location of Beijing.

During the hazy days, the mid-tropospheric westerly flow becomes weaker over the NCP as compared to the clear days (Fig. 2a-c). The mid-tropospheric trough also moves northwards as suggested by the dipole pattern in Fig 2c, which shows the differences in the U_{500} for hazy and clear days. The northerly flow in the lower troposphere is weaker during hazy days as compared to clear days (Fig. 2d-f). The lower troposphere is relatively warmer during hazy days as compared to clear days (Fig. 2g-i) whereas the upper troposphere is cooler over the NCP (Fig. 2j-l). The changes in these variables are also consistent with the previous studies (e.g. Cai et al., 2017) that showed similar changes for this time period. Therefore, we use these four variables for the calculation of the HWI, which is used as a proxy for haze conducive and clear weather conditions under a future climate.

For the calculation of observational HWI, we use ERA-5 reanalysis data for the period 1979-2019. We first create a daily DJF time series of each variable for each reanalyses grid point over China. The daily DJF time series is concatenated for the period 1979-2019. A daily standardised anomaly time series is created for each meteorological variable by first removing the daily mean climatology from each day of the time series and then normalising by the standard deviation. Spatial averages are then obtained over the relevant boxes (B1 to B5) for each meteorological variable following Cai et al. (2017) (Fig. 1). The HWI time-series is calculated by using the following equation:

$$HWI\ (t) = U_{500}\ (t) + V_{850}\ (t) + dT(t)$$

where $U_{500} = U_{500,B1}\ (t) - U_{500,B2}\ (t)$, $V_{850} = V_{850,B3}\ (t)$, and $dT = T_{850,B4}\ (t) - T_{250,B5}\ (t)$. The HWI (t) time series is then itself normalized by its own standard deviation.

For the PPE historical and RCP8.5 simulations, the daily HWI time series is calculated for each ensemble member for DJF for 1969-2089 using the same methodology as used for ERA-5, with the difference being that the normalisation of the PPE time-series (1969-2089) is performed using the historical standard deviation (1969-2005), following Cai et al. (2017). Similarly, the HWI time series is calculated for the PPE pre-industrial control simulations for 170 model years out of 200 model years (the first 30 years are discarded as model spin-up period). The normalisation of the pre-industrial control time series is performed using the standard deviation for 170 years. The pre-industrial control simulations used here are initialised with past forcings corresponding to the year 1900 and therefore are an approximate representation of the internal variability of the current climate as this does not take into account any temporal changes in the internal variability from 1900 to the historical and future periods used here.

3. Haze Weather Index as an indicator for clear and haze conducive weather conditions over the NCP

As the HWI was originally proposed for Beijing by Cai et al. (2018), we first determine if the HWI can be used as a representative of haze conducive and clear weather conditions for the present climate for Beijing using (a) $PM_{2.5}$ concentrations from the US embassy station in Beijing and (b) $PM_{2.5}$ concentrations averaged over larger Beijing domain from CAQRA reanalysis and (c) visibility data from the CMA stations in Beijing. We then determine the spatial extent of the region for which HWI can be used as an indicator of haze conducive and clear weather conditions using $PM_{2.5}$ concentrations for China using CAQRA reanalysis data. We use the 25th and 75th percentile values of daily mean $PM_{2.5}$ concentrations to identify the clear and hazy days, respectively for each dataset. For visibility, we use the opposite criterion, i.e. 25th percentile as a threshold for hazy days and 75th percentile as a threshold of clear days, as lower visibility is associated with hazy days and higher visibility with clear days. The days with daily $PM_{2.5}$ concentration or visibility lying between the 25th and 75th percentile values are identified as moderately polluted days.

3.1 $PM_{2.5}$ concentrations for Beijing versus HWI

We examine the relationship between the daily HWI and $PM_{2.5}$ concentrations for the US embassy station for Beijing. Figure 3 (a) shows that the daily HWI increases linearly with increasing $PM_{2.5}$ concentrations for up to ~150 μg m^{-3} and $PM_{2.5}$ > 150 μg m^{-3}, the HWI starts to level-off (note the log scaling in the y-axis). The time-series correlation between the HWI and $PM_{2.5}$ concentration is ~0.58, which is significant at the 1% level. Callahan et al. (2019) have also obtained a correlation coefficient of 0.58 for daily $PM_{2.5}$ concentrations from the U.S. embassy in Beijing and the HWI calculated using NCAR R1 reanalysis.

The 25th and 75th percentile values of daily mean $PM_{2.5}$ concentrations for the US embassy Beijing station for DJF 2009-2017 are ~35 and ~150 μg m^{-3} respectively. We determine the percentage of hazy days (with daily mean $PM_{2.5}$ concentrations >150 μg m^{-3}) and clear days (with daily mean $PM_{2.5}$ concentrations < 35 μg m^{-3}) for different HWI ranges (Fig. 3e). Out of all days with HWI >1, 64% have daily mean $PM_{2.5}$ concentrations > 150 μg m^{-3} and 98% with $PM_{2.5}$ concentrations >35 μg m^{-3}. This suggests that for HWI >1, almost all days are hazy or moderately polluted. Similarly, almost all days with HWI < -1 are clear or moderately polluted. Using HWI thresholds of ±1 demarcates between the clear and hazy days, i.e. almost no clear days occur for HWI >1 and almost no hazy days occur for HWI <-1.

We have also examined the relationship between the individual variables in the HWI (section 2.2) and $PM_{2.5}$ concentrations observed at the US embassy in Beijing/CAQRA and find that the individual components have correlation values that are similar to or less than that of those used in the combined HWI. Also, physically multiple favourable weather conditions, as represented by each of these variables, collectively provide a conducive setting for haze. Hence, we focus on the HWI as a combined index rather than its individual components.

To examine if the $PM_{2.5}$ concentrations from the US embassy station are sensitive to the abrupt changes in the local meteorology, e.g. wind speeds or direction, we also examine the relationship between the HWI and $PM_{2.5}$ concentrations averaged over the domain centred around Beijing (116.15 – 116.65 °E, 39.65 – 40.15 °N) from the CAQRA reanalysis data (Fig. 3b and 3f). The $PM_{2.5}$ concentrations for region spatially averaged around Beijing from CAQRA data are in the range 6 μg m^{-3} – 441 μg m^{-3} and from the Beijing US embassy station are 6 μg m^{-3} – 569 μg m^{-3} suggesting the values from both data sources are comparable. The correlation coefficient is ~0.58, which is the same as the correlation obtained using the US embassy data. The total number of hazy, clear and moderately polluted days for different HWI ranges also show similar results for both datasets (Fig. 3e-3f). This implies that the HWI relationship with $PM_{2.5}$ concentrations is robust across different data sources and that $PM_{2.5}$ is a regional pollutant.

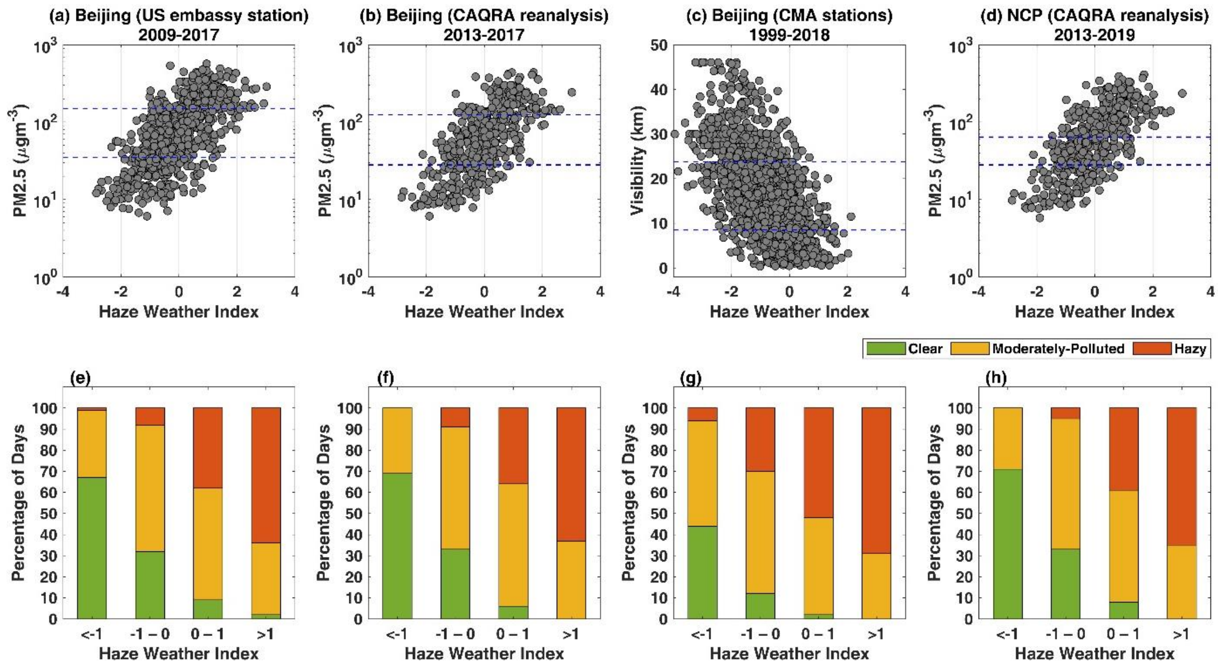

Figure 3 HWI versus daily mean **(a)** $PM_{2.5}$ concentrations for the US embassy Beijing station for DJF 2009-2017 **(b)** $PM_{2.5}$ concentrations spatially averaged over the region around Beijing (116.15-116.65 °E, 39.65 - 40.15 °N) from CAQRA reanalysis for DJF 2013-2017 **(c)** visibility averaged over 20 stations from the CMA for DJF 1999-2018 and **(d)** $PM_{2.5}$ concentrations spatially averaged over the NCP (36-43.5 °N, 107-122 °E) from CAQRA reanalysis. Blue lines show the 25th and 75th percentile thresholds used to define clear and hazy days for each dataset. Percentage of clear, moderately polluted and hazy days for different HWI ranges for the **(e)** US embassy Beijing station for DJF 1999-2018 **(f)** larger Beijing domain (116.15-116.65 °E, 39.65 - 40.15 °N) from CAQRA reanalysis for DJF 2013-2017 **(g)** Beijing for DJF 1999-2018 **(h)** NCP from the CAQRA reanalysis for DJF 2013-2017.

3.2 Visibility for Beijing versus HWI

As visibility is an optical representative of haze (Wang et al., 2006) and the data for visibility is available for a relatively long period (1999-2018) as compared to the $PM_{2.5}$ concentrations, we also correlate the HWI with the visibility over Beijing. Figure 3 (c) shows that the HWI is inversely related to the visibility for the Beijing station. The time-series correlation between the HWI and visibility is -0.63, which is significant at the 1% level. The days with visibility < 8.5 km are identified as hazy days, days with visibility > 23.8 km are identified as clear days. For days with HWI > 1, no clear days occur and similarly for days with

HWI< -1, only 6% of days are hazy (Fig 3g). This further confirms that the correlation between the HWI and haze is significant for a longer period (1999-2018) using visibility as a metric for haze (alternative to the $PM_{2.5}$ concentrations used above).

3.3 $PM_{2.5}$ concentrations over North China Plain versus HWI

We now determine the spatial extent for which HWI can be used as an indicator of haze clear or haze conducive conditions using $PM_{2.5}$ concentrations from CAQRA reanalysis. We correlate the daily time-series of $PM_{2.5}$ concentration at each grid point with the HWI for DJF 2013-2017 (Fig. 4). Over the entire NCP (36-43.5 °N, 107-122 °E), the correlation coefficient between the daily HWI and gridded $PM_{2.5}$ concentration is ~0.7, significant at the 1% level. The correlation is considerably lower but still significant over other eastern China regions, e.g. north easternmost China and the Sichuan Basin (27-32 °N, 102-107 °E).

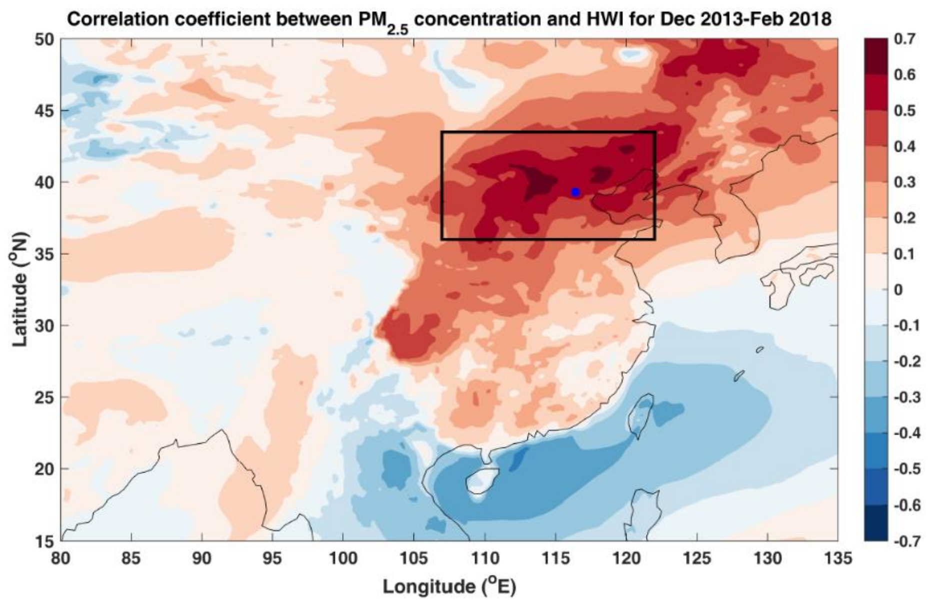

Figure 4 Spatial distribution of correlation between winter $PM_{2.5}$ concentrations and HWI time series at each grid point. Blue dot shows the Beijing station (39.3 °N, 116.4 °E) and the black rectangle shows the North China Plain (36-43.5 °N, 107-122 °E).

Considering daily mean $PM_{2.5}$ concentrations averaged over the NCP, we also find a linear relationship with the daily HWI (r = 0.66; significant at the 1% level; Fig 2d). We also calculate the percentage of clear and hazy days for different HWI ranges for the larger domain of the NCP using the 25th and 75th percentile values, respectively. The percentage of hazy and clear days for HWI > 1 and HWI < -1 for NCP in CAQRA reanalyses are very similar to the values obtained for the US embassy Beijing station (Fig 3h).

Overall, our results confirm that the daily HWI has a robust relationship with daily $PM_{2.5}$ concentrations not only for the Beijing station but across the NCP for the given time periods. Therefore, we use HWI > 1 as a proxy for haze conducive weather and HWI < -1 as a proxy for clear weather across the NCP region. This threshold is also consistent with several other studies (e.g., Cai et al., 2017; Callahan and Mankin, 2020; Callahan et al., 2019), that have used HWI >1, as a cut-off for haze conducive weather for Beijing. We now calculate the frequency of haze conducive weather (HWI >1) and clear weather (HWI <-1) for the past and future using ERA-5 reanalysis and PPE members.

4. Historical and future changes in haze conducive and clear weather occurrence

The frequency of haze conducive weather (HWI >1) and clear weather (HWI <-1) from the ERA-5 reanalyses and the PPE are shown in Fig. 5. For ERA-5, the frequency of haze conducive weather has increased, whereas the frequency of clear weather (HWI<-1) has reduced for the period 1979-2018. The mean frequency of haze conducive weather using 16 PPE members shows a relatively larger increase than ERA-5 for the same 1979-2018 time period (Fig. 5a). In contrast, the mean frequency of clear weather from the PPE for this period shows a similar reduction to that obtained using the ERA-5 reanalyses (Fig. 5b).

We examine the changes in the frequency of haze conducive weather (HWI>1) and clear weather (HWI<-1) for the historical (1979-2005) and three future periods, i.e. near (2006-2032), mid (2033-2059) and far (2060-2086) future. The mean frequency for haze conducive weather is 14.7 days per winter obtained from the ERA-5 reanalysis and 15.0 days per winter from the PPE mean for the historical period. The corresponding values for clear weather are

15.0 days and 15.2 days per winter for ERA-5 and PPE, respectively. This shows a good agreement between the mean frequencies of haze conducive and clear for the ERA-5 data and the PPE mean for the historical period.

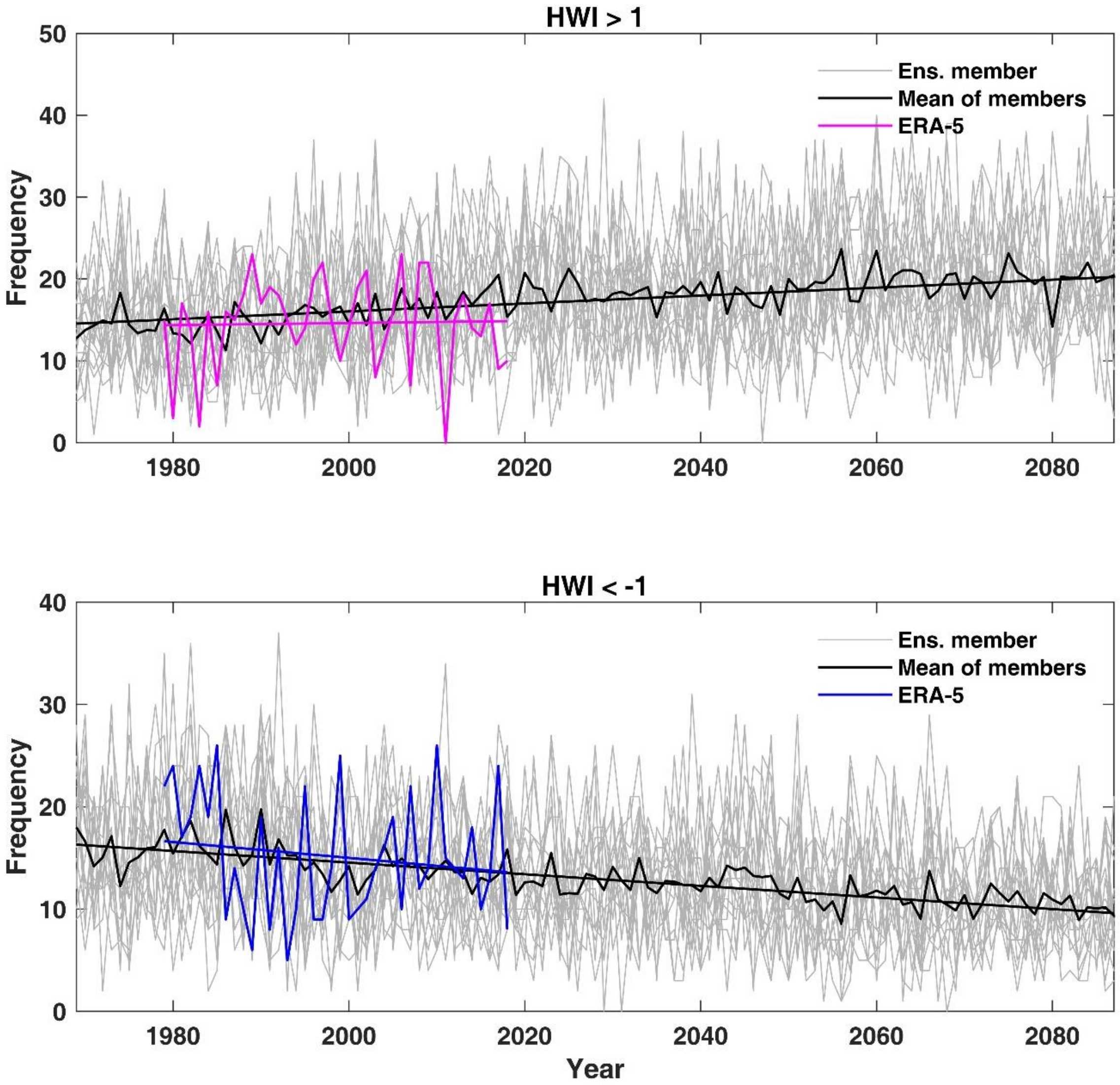

Figure 5 Frequency of haze conducive weather (HWI>1, pink line) and clear weather (HWI<-1, blue line) per winter from ERA-5 reanalysis (1979 to 2018). Year 1979 represents period from 1 December 1979 to 28 February 1980 and so on. For each winter (DJF), we calculate the total number of days with HWI >1 as proxy for haze conducive weather and HWI < -1 as proxy for clear weather conditions. Grey lines show frequencies from 16 individual PPE members and black line shows the mean of frequency using all 16 PPE members for 1969-2087 under the RCP8.5 scenario. Linear trend is calculated using the line of best fit.

The mean frequency of haze conducive weather for near, mid and far future is 17.9, 18.6 and 19.9, respectively. The mean frequency for the same future periods for clear weather is 13.2, 12.2 and 10.8, respectively (Fig. 6a). The mean change in the frequency of haze conducive weather averaged across all PPE members is 20%, 24% and 33% for the near, mid and far future respectively as compared to the historical period, suggesting that the frequency of haze conducive weather will likely increase for all future periods (Fig. 6a). However, there exists a very large range in the projected change for all three future periods suggesting internal variability or parametric effect could influence the future projections of haze conducive weather. For the near and mid future, days with HWI>1 are projected to change by -1% to 41% and -12% to 65% across the 16 PPE members, respectively, as compared to the frequency for the historical period. For the far future, the range of projected change is even larger, and an increase of ~87% in the frequency of haze conducive weather is also possible. It is noted that, for all three periods, only one of the sixteen ensemble members (E16 shown in Fig. 10) shows a reduction in the haze conducive weather frequency whereas other ensemble members show an increase in frequency for all periods. For the historical period, E16 ensemble member has a mean frequency of 16.3, which reduces to 16.2, 14.4 and 15.2 for near, mid and far future. While E16 ensemble member shows a consistent reduction in mean frequency in future, the reduction is specific to only this ensemble member and is not a general feature across PPE members.

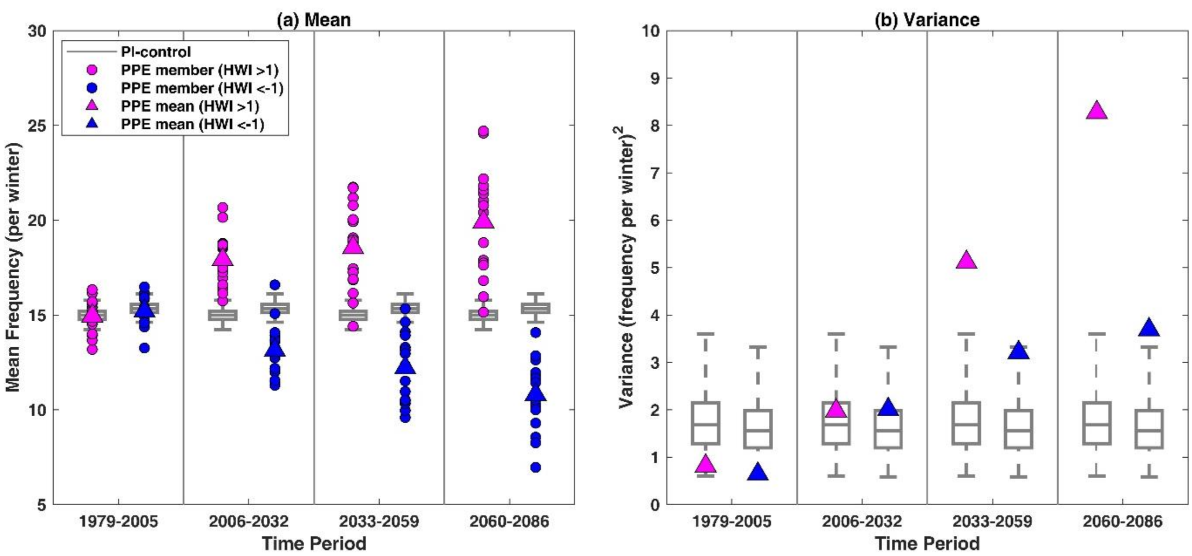

Figure 6 (a) Mean frequency of haze conducive weather (HWI>1, pink) and clear weather (HWI<-1, blue) for the historical period (1979-2005), near (2006-2032), mid (2033-2059) and far (2060-2086) future under the RCP8.5 scenario. Circles represent PPE members and triangles PPE mean. Grey box and whiskers show the distribution of 10,000 values of mean frequencies sub-sampled from the control simulation, **(b)** same as (a) but shows variance across 16 PPE members for each period. For box and whiskers, we first randomly sampled 10,000 time series of length 27 years using 2704 years of pre-industrial control simulation and calculated 10,000 values of mean frequency. We then randomly sub-sample 16 mean values (corresponding to the number of ensemble members) from the 10,000 mean values, calculated their mean for (a) and variance for (b). This is repeated 10,000 to obtain a distribution. The boxes are at the 25th and 75th percentile and the whiskers at 2.5th and 97.5th percentile of mean and variance distribution. For panel (a), the box and whiskers are comparable only to the ensemble means (triangles) and not ensemble members (circles).

For clear weather (HWI<-1), the mean change in the frequency averaging across all PPE members is -13%, -20% and -29% for near, mid and far future, respectively (Fig 6a). Considering the range across the 16 PPE members, the frequency of clear weather for near, mid and far future is projected to change by -29% to 25%, -36% to 10% and -57% to -9%, respectively. Overall, most ensemble members show an increase in the frequency of haze conducive weather and a reduction in the frequency of clear weather for all three future periods. However, negligible change or even the opposite change, though less likely, but possible for all periods.

We also determine the influence of anthropogenic climate change and the parametric effect on the frequencies of haze conducive weather (HWI>1) and clear weather (HWI<-1) for the historical as well as the three future periods. As shown in later Section 5, the estimate of interannual variance from the control is representative of all time periods and shows no discernible parametric effect. Therefore, we pool the 16 PPE control simulations to sample the internal variability for box and whiskers shown in Fig. 6 (a) and 6 (b) (see captions for details on resampling).

In Fig. 6 (a), we show the mean frequency of haze conducive weather and clear weather for 16 individual PPE members (circles) and PPE mean (triangles). The grey box and whiskers represent the range of ensemble mean frequencies that can be explained by the internal variability. If the PPE mean (triangles) lies within the whiskers (i.e. 95 percentile of the control distribution) we conclude no influence of anthropogenic climate change on mean frequency however if the PPE mean lies outside the whiskers, it would represent a climate change signal in the mean frequency. Figure 6 (a) suggest that the mean frequencies for haze conducive as well as clear weather lies within the box-whiskers for the historical but lies outside the whiskers for the three future periods, thereby showing a clear impact of anthropogenic climate change on the frequencies of both haze conducive and clear weather conditions.

We now examine whether the differences in the mean frequency across different PPE members (shown by circles in Fig. 6a) for a given period can be explained by the internal variability or if the differences in PPE members partly arise due to the parametric effect. The triangles in Fig. 6b shows the variance across 16 PPE members, i.e. variance across 16 circles shown in Fig. 6a, for each time period. The whiskers in Fig. 6b show the 95^{th} confidence interval from the control simulation and is representative of the internal variability. For any time period, if the PPE member variance (triangle) lies within the whiskers, we conclude that the differences in mean frequencies in Fig. 6a can be fully explained by the internal variability and there is no discernible impact of the parametric effect. However, if the triangles lie outside the whiskers in Fig. 6b, we conclude an impact of the parametric effect on the mean frequency for that period. For the points that lie outside the whiskers in Fig. 6b, we also quantify the percentage of variance that can be explained by the internal variability and parametric effect. For any time period, the variance in ensemble mean due to the parametric effect is simply calculated as follow and the remaining variance is attributed to the internal variability.

$$\frac{\text{Total variance in the ensemble mean} - \text{Mean variance from the control simulation}}{\text{Total variance in the ensemble mean}} \times 100$$

Figure 6b shows that the difference in mean frequencies across PPE members (as shown by PPE member variance) is small for the historical and near future but increases for mid and far future periods. For the historical and near future periods, the PPE member variance lies within the range sampled by the internal variability for both haze conducive weather (HWI>1) and clear weather (HWI<-1). This shows that there is no discernible influence of the parametric effect on the frequency of haze conducive weather or clear weather conditions for the historical and near future periods.

For mid-future, the PPE member variance for clear weather lies within the whiskers and therefore no discernible influence of the parametric effect is detected. In contrast, the PPE member variance for haze conducive weather lies outside the whiskers and the internal variability can explain ~33% of the variance across PPE members and the remaining ~67% arises due to the parametric effect.

For the far future, triangles corresponding to both haze conducive and clear weather lies well outside the whiskers and therefore show a clear influence of parametric effect. Only ~20% of the variance in the frequency of haze conducive weather and ~43% variance in the frequency of clear weather can be explained by the internal variability and the remaining 80% and 57% respective variance in the frequencies arise due to the parametric effect.

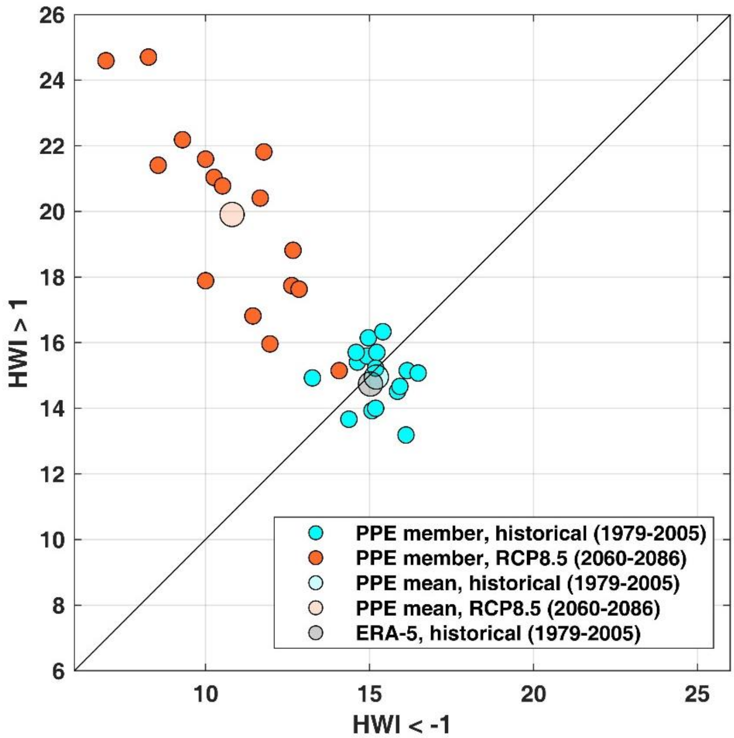

Figure 7 Frequency of haze conducive weather (HWI>1) versus clear weather (HWI<-1) averaged over the historical period (1979-2005) and the far-future (2060-2086) period under RCP8.5 using all PPE members. Circles denote individual PPE members whereas triangles denote the mean of the members. Grey triangle shows mean frequency from ERA-5 reanalysis for the historical period (1979-2005). The black solid line shows the 1:1 (identity) line.

In addition to the changes in the frequencies over time, we also investigate the relative changes in the frequency of haze conducive weather (HWI>1) versus clear weather (HWI<-1). The average haze conducive and clear weather frequency over the historical period are almost equal for each PPE member (Fig. 7). All PPE members show a higher frequency for haze conducive weather than clear weather under the far future (2060-2085), however, there exists a substantial range in this change. The frequency of winter haze conducive weather can be similar or up to 3.5 times the frequency of clear weather conditions (Fig. 7). Similar results are also obtained for the near and mid-future. Averaged across the PPE members, the number of haze conducive days can increase by ~2 times as compared to the number of clear days in future. As noted in Fig. 7, the spread in the haze conducive weather frequency amongst individual ensemble members is also larger for the far future (2060-2086) compared to the historical period. This suggests a larger uncertainty and a larger range of possible future meteorological conditions affecting haze and air quality as compared to the historical period. Other studies have (e.g., Cai et al., 2017; Callahan and Mankin, 2020) also found similar increases in the frequency of haze conducive weather for the future. However, the range of projected change differs substantially across models as well as ensemble members. In our study, in addition to the frequency of haze conducive weather, we also evaluate the changes in the frequency of clear weather across different future periods and compared the relative changes in both the frequencies, which is not examined in the past studies.

We now investigate changes in the distribution of the HWI as well as individual constituents of the HWI between the far future (2060-86) and the historical (1979-2005) period. The probability distribution of the HWI shows a shift in the distribution towards higher magnitudes for the far future as compared to the historical period (Fig. 8). This implies an increased frequency of haze conducive weather, as the number of days with HWI >1 increase. A similar shift is apparent in the zonal-mean wind (U_{500}) and the vertical temperature profiles (dT), whereas no apparent shift is noted in V_{850}. We also find that the shift in the HWI, as well as U_{500} and dT distribution, is not due to the shift in one particular PPE member or time period. It is consistent across the 16 PPE members and is continual over time from the historical to the far-future period. Therefore, for the PPE analysed here, the changes in the haze conducive weather (HWI>1) is largely associated with the changes in the U_{500} and dT, and V_{850} appear to have a less important role. Despite using a multimodel ensemble and a different time period than used here, a similar result with a relatively larger shift in the PDFs of U_{500} and dT as compared to V_{850} can also be noted in the Cai et al. (2017).

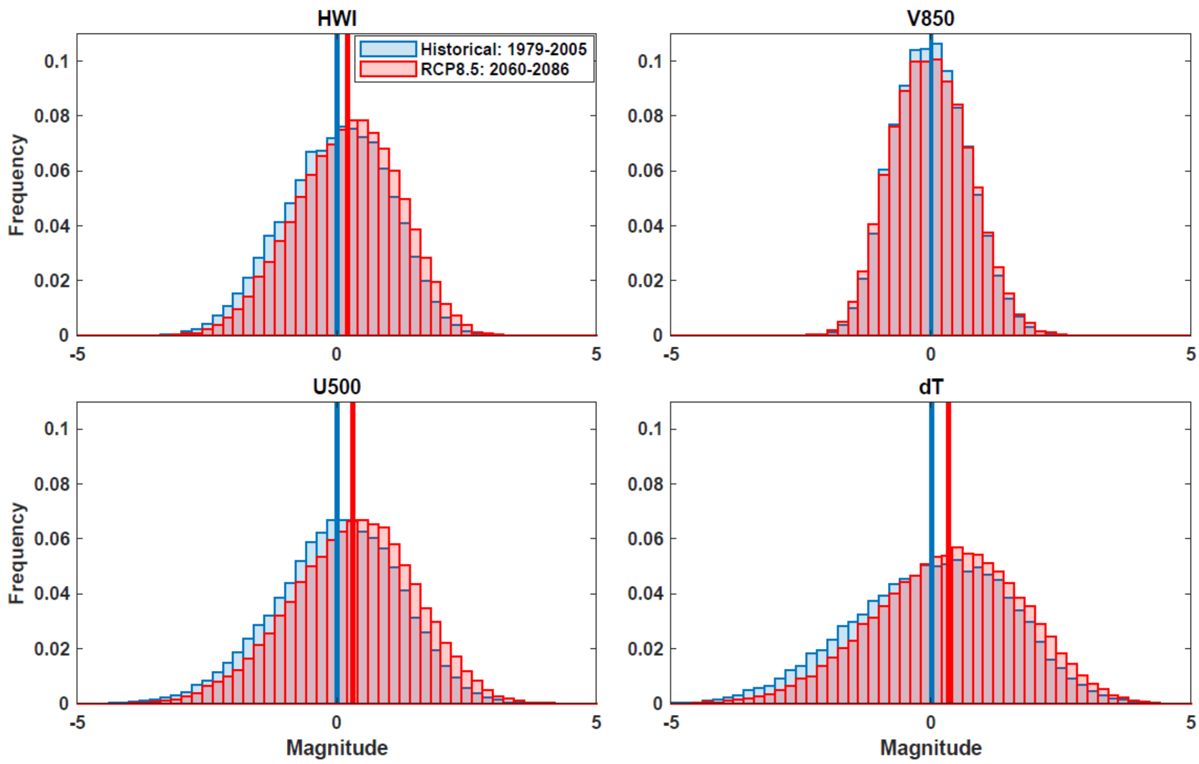

Figure 8 Probability Distribution Functions (PDF) for the winter HWI, meridional winds at 850 hPa pressure level (V_{850}), zonal winds at 500 hPa pressure level (U_{500}) and temperature gradient between the lower and upper troposphere (dT). The PDF for the HWI is created using the daily DJF time series of all 16 PPE members. PDFs for V_{850}, U_{500} and dT are created using the normalized daily DJF time series of each variable calculated for the HWI (see section 2.2 for details) and represents the constituent variables of the HWI. Blues bars show the PDFs for the historical period and red for the far future under the RCP 8.5 scenario. Blue and red solid lines show the mean values of the PDF for historical and far future, respectively.

5. Interannual variability in haze conducive and clear weather frequency

Large interannual variability in the frequency of haze conducive (HWI>1) and clear weather (HWI<-1) is apparent in both individual PPE members and ERA-5 reanalysis (Section 4). Therefore, we examine the changes in the interannual variance of the frequencies for future periods as compared to the historical period. We also compare the variance in historical and future time periods with the variance in the control simulation to discern the influence of the model physical parameterisations, i.e. parametric effect, on the variance.

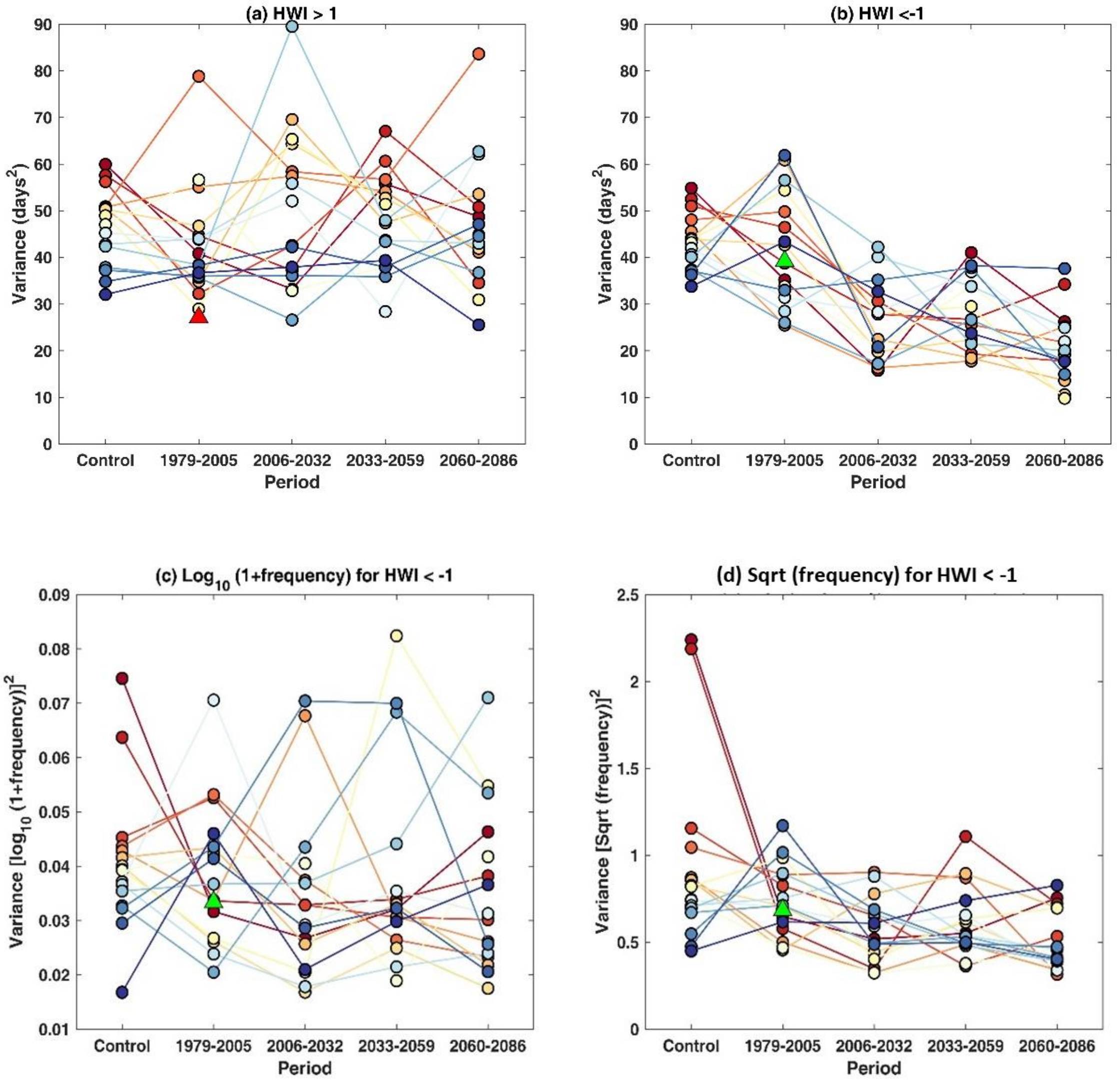

Figure 9 Interannual variance in frequency of winter **(a)** haze conducive weather (HWI>1) and **(b)** clear weather (HWI<-1) for the control simulation, historical (1979-2005), and near (2006-2032), mid (2033-2059) and far-future (2060-2086) under RCP8.5 for all 16 PPE members. Coloured circles are for individual PPE members and triangles for ERA-5 reanalysis. **(c-d)** are same as **(b)** but with $\log_{10}$ and square root power transformations. For (c-d), we first calculate the $\log_{10}$ of (1+frequency) and square-root of the frequency of clear days for the control simulation and each time-period, and then estimate variance for each respective period. The length of control simulation and all future periods is the same as historical, i.e. 27 years. The 27 years used for control here are randomly selected from 170-year control simulation for each member.

The interannual variance for ERA-5 data is 27 days^2 and 39 days^2 for haze conducive and clear weather, respectively, for the historical period (1979-2005) (triangles in Fig. 9a-b). The interannual variance in haze conducive weather frequency derived from the PPE members for the historical period is larger than that for the ERA-5, whereas for the clear weather the variance for ERA-5 lies within the range of the PPE members. No consistent change in the interannual variance of haze conducive weather is noted for any of the PPE members (note the changes in colour ranking) from the historical to the future periods suggesting little influence of the parametric effect on the interannual variance of haze conducive weather.

In contrast, the frequency of clear weather for most PPE members show a marked reduction in the interannual variance from historical to near-future (Fig. 9b). However, as the frequency of clear weather show a decreasing trend in time (see Fig. 5b), the mean frequency would be expected to reduce for the three future periods. Also, the reduction in variance could arise as the frequencies of clear weather approach their lower bound of zero. With count data, a power transformation is often applied to stabilize the variance across all time periods. We applied two power transformations, i.e. $\log_{10}(1+x)$ and square-root (x), where x is the count data (Fig. 9c-d). We find the spread in the variance in the control simulation across the PPE members is comparable with the historical as well as future periods (Fig. 9c-d). Note that for control simulation we randomly selected 27 years (length same as historical and future periods) from 170 years of control simulation from each PPE member, however, we note comparable variance for the other randomly selected samples. Figure 9 (c-d) also shows that the individual PPE members show inconsistent changes in the variance (noting changes in the colour ranking) from control to historical and future periods. Therefore, no robust changes in the interannual variance of haze conducive and clear weather can be detected from control to historical and future periods. This means we can use the variance in the control simulation as a representative estimate of internal variability. This enables us to quantify the influence of the parametric effect and anthropogenic climate change on the mean frequencies (see previous section) and trends in frequencies (see next section) across different periods.

6. Influence of the anthropogenic climate change and parametric effect on trends

We discern the influence of the anthropogenic climate change and parametric effect on the future projections of the trends in the frequency of haze conducive weather (HWI >1) and clear weather (HWI <-1). The time series of the haze conducive and clear weather frequency from ERA-5 and the 16 PPE members for the historical and future periods is shown in Fig. 11 (a) and 11 (b). The 95th percentile values (blue shaded region) and the range (blue dotted lines) in the haze conducive and clear weather frequency from the respective control simulation for each PPE member are also shown.

For haze conducive weather (HWI>1), the time series for selected PPE members (e.g. E3, E4) show increasing positive trends. In particular, towards the end of the 21st century (Fig. 10a), the lower half of the control range is seldom sampled and more than the expected number of values lie above the 97.5th percentile of the control frequencies. In contrast, for other PPE members (e.g. E8, E10), the full time series sample the control distribution evenly throughout the full period. For clear weather (HWI<-1), some members (e.g. E3, E4) show a clear reduction during the 21st century whilst others (e.g. E16) show no trend and explore the control distribution evenly (Fig 10b).

In Section 4, we examined the influence of anthropogenic climate change and parametric effect on the mean frequencies. The analysis of mean frequencies provides an estimate of the accumulated influence of climate change on frequencies with respect to the control simulations whereas analysis of trends would provide a better estimate of changes within a selected time period. Therefore, we apply the same analysis on the trends in the frequencies (Fig. 11).

(a) HWI>1

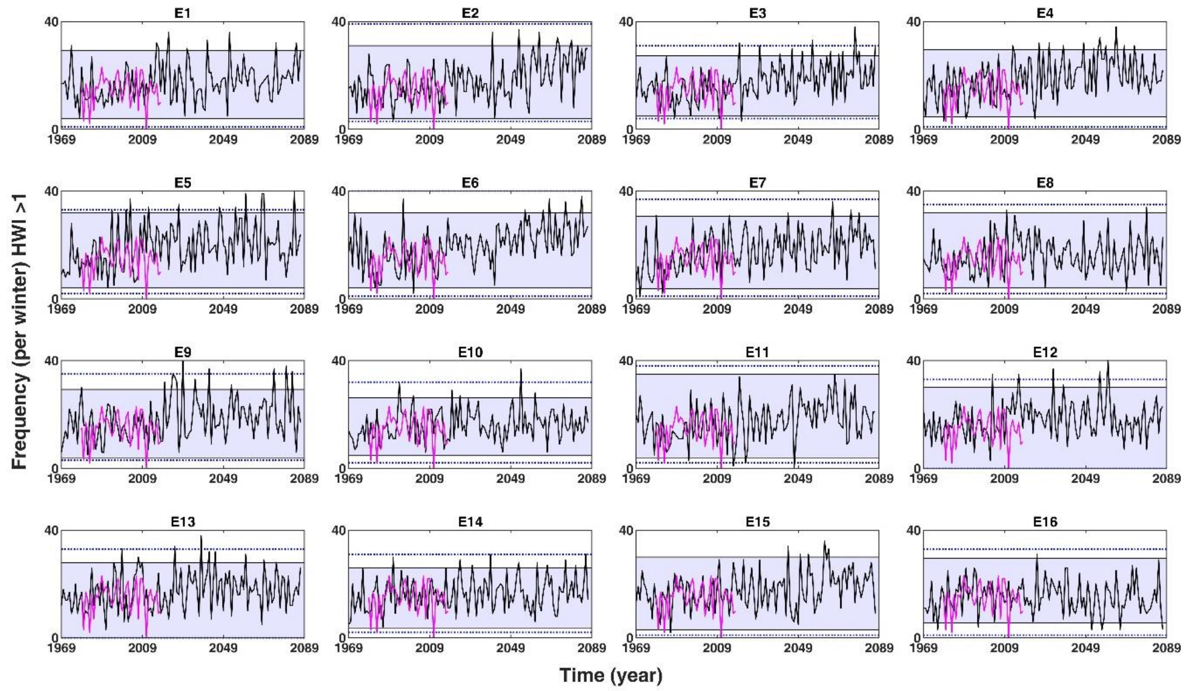

(b) HWI<-1

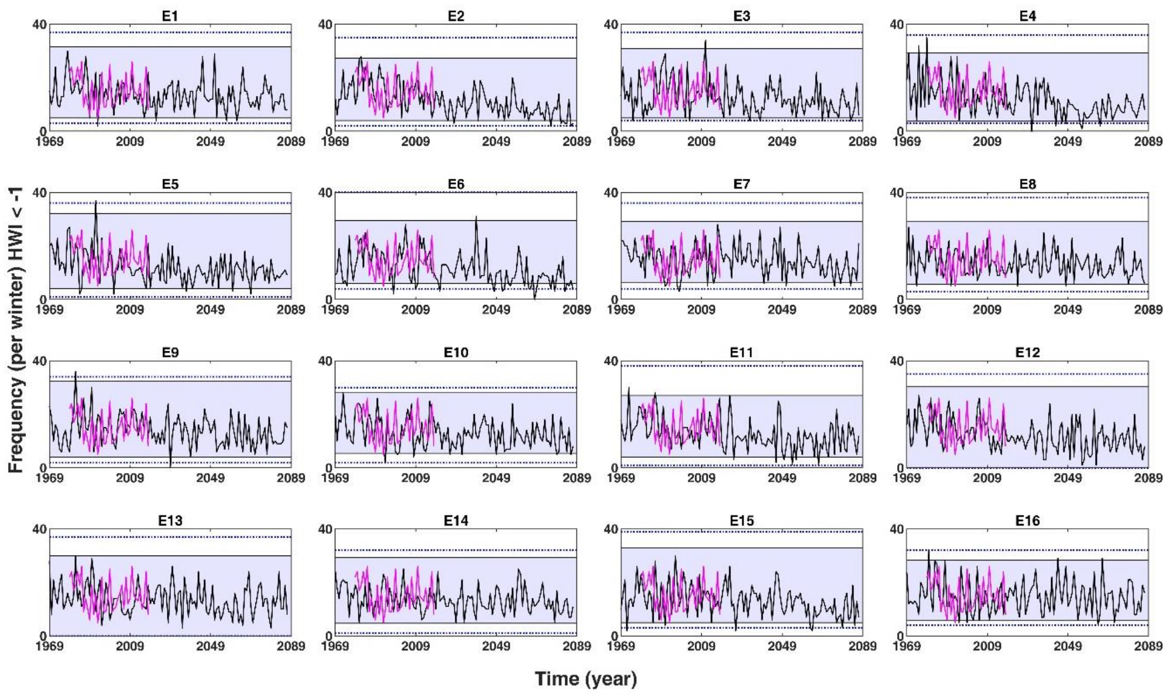

Figure 10 Frequency of **(a)** haze conducive weather (HWI>1) and **(b)** clear weather (HWI<-1) per winter for individual PPE members (black line) under the historical and RCP8.5 scenarios for 1969-2087 and ERA5 reanalysis (pink line) for 1979-2018. Blue shaded region shows the 95th confidence

interval and blue dashed line shows the range of the frequency of haze conducive and clear weather for the pre-industrial control simulation of 170-years.

We calculate the ensemble mean trend obtained from the 16 individual PPE member trends to determine the influence of climate change for the historical period (see captions of Fig. 11 for details). We describe the evolution of the historical trend for three equal-length future time periods (i.e. near, mid and far future) and examine if the historical trends are sustained across the 21st century and if the trends are discernible outside the range described by the internal variability (Fig. 11a-b). The grey whiskers in Fig. 11 (a) and (b) cover the range of trends that can be explained by internal variability and any trend values lying outside the grey whiskers represent the influence of anthropogenic climate change.

The mean trend in the frequency of both haze conducive (HWI>1) and clear weather (HWI <-1) for the historical period (1979-2005) lie outside the 95% confidence interval of the control simulations. This suggests that the trends noted for the historical period cannot be explained by internal variability alone and there is a substantial impact of anthropogenic climate change on the historical trends. The trends in haze conducive weather lie within the envelope of internal variability for the three future periods analysed here implying that the historical trend is not sustained over the 21st century and indistinguishable from the internal variability for the future. Figure 11 (a) also shows a positive mean trend in haze conducive weather (HWI>1) for historical, near and mid future, but a weak negative trend for far future. While the frequency of haze conducive weather increases for all three future periods with respect to the historical period as shown in Fig. 6a, the trends only show an increment or reduction for that period as these are not referenced to the historical period. Therefore, trends could still be negative within any selected period, as in the case of the far future. In contrast, the mean trends in clear weather frequency for near (2006-2032) and mid future (2033-2059) lie outside the 95% confidence interval of the control simulation. This shows that for clear weather frequency (HWI<-1), the historical trend is sustained over the first half of the 21st century and then it levels off.

We now examine the influence of the parametric effect on the trends in the frequency of haze conducive and clear weather. In Fig. 11 (c) and (d), we show the variance in trends for the time series resampled using the control simulation (see captions for details on resampling). The grey box and whiskers show the 95th confidence interval of the control variance used to represent the internal variability. The variance in PPE trends calculated using 16 PPE members for selected time periods is overlaid (circles). In Fig. 11 (c-d), if the variance for historical or future periods lies outside the whiskers, we conclude an impact of the parametric effect on the trends. However, if the variance across the 16 PPE members lies within the whiskers, we conclude no impact of the parametric effect on the trend. Note that the variance in trends for clear weather is in log-transformed space. As can be seen in Fig. 11c and 11d, the variance in PPE trends for historical and future periods lies within the 95th percentile distribution of the internal variability for both haze conducive and clear weather. Therefore, we do not find any discernible influence of the parametric effect on the trends in the frequencies.

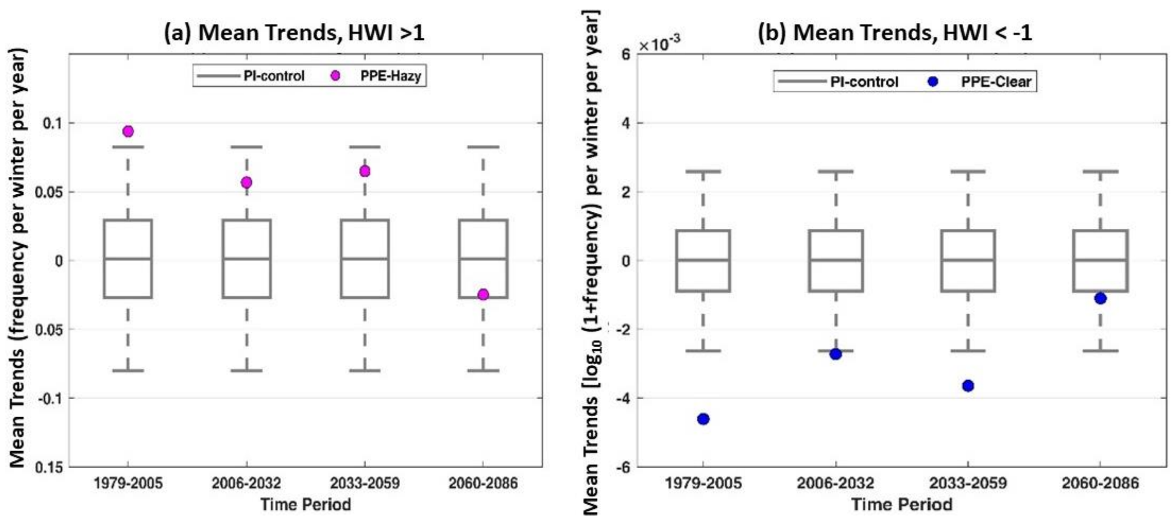

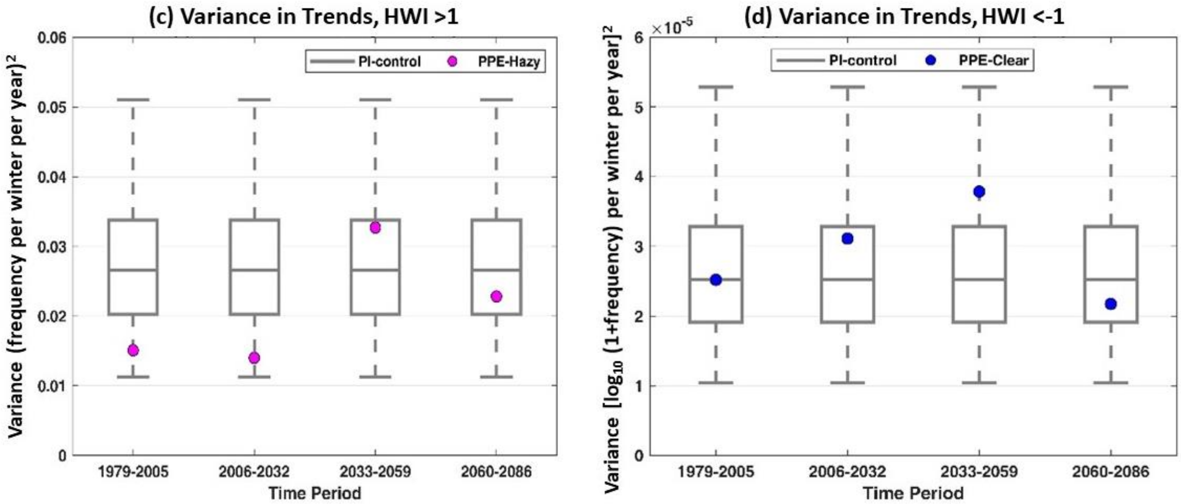

Figure 11 Mean PPE trends for the frequency of **(a)** haze conducive weather (HWI>1) and **(b)** clear weather (HWI<-1) for winter. Circles show the mean trends from 16 PPE members for the historical (1979-2005) and near (2006-2032), mid (2033-2059) and far (2060-2086) future under the RCP8.5 scenario. Grey box and whiskers show the distribution of 10,000 values of trends sub-sampled from the control simulation. **(c-d)** same as (a-b) but mean is replaced by variance in trends. For box and whiskers, we first randomly sampled 10,000 time series of length 27 years using 2704 years of pre-industrial control simulation and calculated 10,000 values of trends. We then randomly sub-sample 16 trends values from the 10,000 trend values and calculate the variance and mean of 16 trend values. The boxes are at the 25th and 75th percentile and the whiskers at 2.5th and 97.5th percentile of mean and variance distribution. For clear days, the frequencies were transformed to log space by applying a power transformation of $\log_{10}$ (1+ frequency) before calculating trends.

7. Conclusions

In this study, we elucidate for the first time the influence of model physical parametrisations, in addition to internal variability and climate change, on the future haze conducive and clear weather conditions over the North China Plain (NCP) using the Perturbed Parameter Ensemble (PPE) from the Met Office HadGEM3-GC3.05 model. We examine the changes in winter (December-February) haze conducive and clear weather conditions for past and future over the NCP using a large-scale meteorology-based daily Haze Weather Index (HWI). We first identify the regional extent of the application of the HWI over China. We find that the HWI >1 can be used as an indicator of haze conducive weather conditions and HWI<-

1 as an indicator of clear weather conditions for the entire NCP due to the spatial coherence of regional meteorological conditions over this region.

The PPE shows that under the RCP8.5 emission scenario, the mean frequency of haze conducive weather (HWI>1) can increase by up to ~65% in the near (2006-2032) and mid (2033-2059) future and by ~87% in far future (2060-2086) as compared to the historical period (1979-2005). In contrast, the frequency of clear weather (HWI<-1) can reduce by up to ~40% in the near and mid-future and by ~57% in the far future. However, the opposite change of relatively lower magnitude or negligible change in frequency of haze conducive and clear weather, though less likely, is possible. The absolute number of days with haze conducive weather in the far future can remain the same or up to ~3.5 times higher than the clear weather over the NCP. There also exist a large interannual variability in the frequency of haze conducive and clear weather conditions. However, no systematic change in the interannual variance of the frequencies is noted in future as compared to the historical period. We also find that enhanced vertical thermal stability due to the warming of the troposphere and weaker northwesterlies over the NCP in the mid troposphere will collectively lead to more frequent haze conducive weather over the NCP. We find a consistently growing influence of anthropogenic climate change and parametric effect on the mean haze conducive and clear weather frequencies across the 21st century. This suggests that in addition to the internal variability, the parametric effect adds as an additional source of uncertainty in future projections of haze conducive and clear weather, particularly towards the end of the 21st century. We find that the impact of anthropogenic climate change is discernible in trends for the historical period for haze conducive weather and up to mid of the 21st century for clear weather. Beyond these periods, the historical trends are not sustained and not distinguishable from the internal variability.

This study considers four atmospheric variables to examine the changes in future haze conducive and clear weather conditions, however, other atmospheric variables (e.g., boundary layer height) or processes may influence the occurrence of haze. Furthermore, even though our study shows the potential for an increase in haze conducive weather conditions and a reduction in clear weather conditions for the future periods, the actual formation of haze will depend on future emissions of air pollutants and their precursors. If the source emissions are cut-off or reduced in the future, the risk of haze formation would naturally reduce. Nevertheless, the projections of changes in the frequency and interannual variance in haze conducive weather conditions can be very useful for developing successful adaptation and mitigation policies for the future that consider both emissions and climate change, and therefore can be beneficial for near and long-term planning and decision-making in relation to improving future $PM_{2.5}$ air quality.

Data Availability

The Copernicus Climate Change Service (C3S) (2017): ERA5: Fifth generation of ECMWF atmospheric reanalyses of the global climate data are available through Copernicus Climate Change Service Climate Data Store (CDS) (https://cds.climate.copernicus.eu/). The PM2.5 concentrations for the US Embassy station in Beijing are archived at the following website (http://www.stateair.net/web/historical/1/1.html). The haze weather index time series for PPE and visibility data used in this paper can be obtained from the authors. The CAQRA dataset can be freely downloaded at https://doi.org/10.11922/sciencedb.00053.

Author Contribution

SJ and RMD conceived and designed the manuscript; DS conducted PPE simulations using Met Office HadGEM model; LP provided the visibility data; SJ performed data analysis,

produced figures, wrote the first draft; all co-authors provided comments on the manuscript and contributed to writing.

Competing interests

The authors declare no financial or non-financial conflict of interest.

Acknowledgements

We thank Dr Li Ke for the discussion on the HWI calculation and Dr Peiqun Zhang for the discussion on severe haze episodes in China. This work and its contributors (SJ, RMD, DS, ST, ZS) were supported by the UK-China Research & Innovation Partnership Fund through the Met Office Climate Science for Service Partnership (CSSP) China as part of the Newton Fund (Met Office Reference Number: DN37368). RD and ZS also acknowledge NERC for funding under the Atmospheric Pollution and Human Health Programme: Grant Nos. NE/N006941/1 and NE/N007190/1. CL was supported by the National Key Research and Development Program of China (Grant No. 2018YFA0606501). We also thank the two reviewers for their constructive comments and suggestions on this manuscript.

References

An, Z., Huang, R. J., Zhang, R., Tie, X., Li, G., Cao, J., Zhou, W., Shi, Z., Han, Y., Gu, Z., and Ji, Y.: Severe haze in northern China: A synergy of anthropogenic emissions and atmospheric processes, Proc Natl Acad Sci U S A, 116, 8657-8666, 10.1073/pnas.1900125116, 2019.

Bai, N., Khazaei, M., van Eeden, S. F., and Laher, I.: The pharmacology of particulate matter air pollution-induced cardiovascular dysfunction, Pharmacology & therapeutics, 113, 16-29, 2007.

Cai, W., Li, K., Liao, H., Wang, H., and Wu, L.: Weather conditions conducive to Beijing severe haze more frequent under climate change, Nature Climate Change, 7, 257-262, 10.1038/nclimate3249, 2017.

Callahan, C. W., Schnell, J. L., and Horton, D. E.: Multi-index attribution of extreme winter air quality in Beijing, China, Journal of Geophysical Research: Atmospheres, 124, 4567-4583, 2019.

Callahan, C. W., and Mankin, J. S.: The Influence of Internal Climate Variability on Projections of Synoptically Driven Beijing Haze, Geophysical Research Letters, 47, 10.1029/2020gl088548, 2020.

Chen, H., and Wang, H.: Haze days in North China and the associated atmospheric circulations based on daily visibility data from 1960 to 2012, Journal of Geophysical Research: Atmospheres, 120, 5895-5909, 2015.

Deser, C., Knutti, R., Solomon, S., and Phillips, A. S.: Communication of the role of natural variability in future North American climate, Nature Climate Change, 2, 775-779, 2012.

Deser, C., Phillips, A. S., Alexander, M. A., and Smoliak, B. V.: Projecting North American climate over the next 50 years: Uncertainty due to internal variability, Journal of Climate, 27, 2271-2296, 2014.

Han, Z., Zhou, B., Xu, Y., Wu, J., and Shi, Y.: Projected changes in haze pollution potential in China: an ensemble of regional climate model simulations, Atmospheric Chemistry and Physics, 17, 10109-10123, 10.5194/acp-17-10109-2017, 2017.

Hawkins, E., and Sutton, R.: Time of emergence of climate signals, Geophysical Research Letters, 39, n/a-n/a, 10.1029/2011gl050087, 2012.

He, J., Yu, Y., Xie, Y., Mao, H., Wu, L., Liu, N., and Zhao, S.: Numerical model-based artificial neural network model and its application for quantifying impact factors of urban air quality, Water, Air, & Soil Pollution, 227, 1-16, 2016.

Hersbach, H., Bell, B., Berrisford, P., Hirahara, S., Horányi, A., Muñoz-Sabater, J., Nicolas, J., Peubey, C., Radu, R., Schepers, D., Simmons, A., Soci, C., Abdalla, S., Abellan, X., Balsamo, G., Bechtold, P., Biavati, G., Bidlot, J., Bonavita, M., Chiara, G., Dahlgren, P., Dee, D., Diamantakis, M., Dragani, R., Flemming, J., Forbes, R., Fuentes, M., Geer, A., Haimberger, L., Healy, S., Hogan, R. J., Hólm, E., Janisková, M., Keeley, S., Laloyaux, P., Lopez, P., Lupu, C., Radnoti, G., Rosnay, P., Rozum, I., Vamborg, F., Villaume, S., and Thépaut, J. N.: The ERA5 global reanalysis, Quarterly Journal of the Royal Meteorological Society, 146, 1999-2049, 10.1002/qj.3803, 2020.

Hong, C., Zhang, Q., Zhang, Y., Davis, S. J., Tong, D., Zheng, Y., Liu, Z., Guan, D., He, K., and Schellnhuber, H. J.: Impacts of climate change on future air quality and human health in China, Proceedings of the National Academy of Sciences, 116, 17193-17200, 2019.

Hou, P., and Wu, S.: Long-term changes in extreme air pollution meteorology and the implications for air quality, Scientific reports, 6, 1-9, 2016.

Jia, B., Wang, Y., Yao, Y., and Xie, Y.: A new indicator on the impact of large-scale circulation on wintertime particulate matter pollution over China, Atmospheric Chemistry and Physics, 15, 11919-11929, 2015.

Kan, H., London, S. J., Chen, G., Zhang, Y., Song, G., Zhao, N., Jiang, L., and Chen, B.: Differentiating the effects of fine and coarse particles on daily mortality in Shanghai, China, Environment international, 33, 376-384, 2007.

Kan, H., Chen, R., and Tong, S.: Ambient air pollution, climate change, and population health in China, Environment international, 42, 10-19, 2012.

Kay, J. E., Deser, C., Phillips, A., Mai, A., Hannay, C., Strand, G., Arblaster, J. M., Bates, S., Danabasoglu, G., and Edwards, J.: The Community Earth System Model (CESM) large ensemble project: A community resource for studying climate change in the presence of internal climate variability, Bulletin of the American Meteorological Society, 96, 1333-1349, 2015.

Knutti, R., Furrer, R., Tebaldi, C., Cermak, J., and Meehl, G. A.: Challenges in combining projections from multiple climate models, Journal of Climate, 23, 2739-2758, 2010.

Kong, L., Tang, X., Zhu, J., Wang, Z., Li, J., Wu, H., Wu, Q., Chen, H., Zhu, L., and Wang, W.: A 6-year-long (2013–2018) high-resolution air quality reanalysis dataset in China based on the assimilation of surface observations from CNEMC, Earth System Science Data, 13, 529-570, 2021.

Li, K., Liao, H., Cai, W., and Yang, Y.: Attribution of Anthropogenic Influence on Atmospheric Patterns Conducive to Recent Most Severe Haze Over Eastern China, Geophysical Research Letters, 45, 2072-2081, 10.1002/2017gl076570, 2018.

Li, Q., Zhang, R., and Wang, Y.: Interannual variation of the wintertime fog–haze days across central and eastern China and its relation with East Asian winter monsoon, International Journal of Climatology, 36, 346-354, 2016.

Liu, C., Zhang, F., Miao, L., Lei, Y., and Yang, Q.: Future haze events in Beijing, China: When climate warms by 1.5 and 2.0°C, International Journal of Climatology, 40, 3689-3700, 10.1002/joc.6421, 2019.

Liu, Q., Jia, X., Quan, J., Li, J., Li, X., Wu, Y., Chen, D., Wang, Z., and Liu, Y.: New positive feedback mechanism between boundary layer meteorology and secondary aerosol formation during severe haze events, Scientific reports, 8, 1-8, 2018.

Liu, T., Gong, S., He, J., Yu, M., Wang, Q., Li, H., Liu, W., Zhang, J., Li, L., Wang, X., Li, S., Lu, Y., Du, H., Wang, Y., Zhou, C., Liu, H., and Zhao, Q.: Attributions of meteorological and emission factors to the 2015 winter severe haze pollution episodes in China's Jing-Jin-Ji area, Atmospheric Chemistry and Physics, 17, 2971-2980, 10.5194/acp-17-2971-2017, 2017.

Pei, L., Yan, Z., Sun, Z., Miao, S., and Yao, Y.: Increasing persistent haze in Beijing: potential impacts of weakening East Asian winter monsoons associated with northwestern Pacific sea surface temperature trends, Atmospheric Chemistry and Physics, 18, 3173-3183, 2018.

Pendergrass, D., Shen, L., Jacob, D., and Mickley, L.: Predicting the impact of climate change on severe wintertime particulate pollution events in Beijing using extreme value theory, Geophysical Research Letters, 46, 1824-1830, 2019.

Petäjä, T., Järvi, L., Kerminen, V.-M., Ding, A., Sun, J., Nie, W., Kujansuu, J., Virkkula, A., Yang, X., and Fu, C.: Enhanced air pollution via aerosol-boundary layer feedback in China, Scientific reports, 6, 1-6, 2016.

Qiu, L., Yue, X., Hua, W., and Lei, Y.-D.: Projection of weather potential for winter haze episodes in Beijing by 1.5 °C and 2.0 °C global warming, Advances in Climate Change Research, 11, 218-226, 10.1016/j.accre.2020.09.002, 2020.

Renhe, Z., Li, Q., and Zhang, R.: Meteorological conditions for the persistent severe fog and haze event over eastern China in January 2013, Science China Earth Sciences, 57, 26-35, 2014.

Sexton, D. M., McSweeney, C. F., Rostron, J. W., Yamazaki, K., Booth, B. B., Murphy, J. M., Regayre, L., Johnson, J. S., and Karmalkar, A. V.: A perturbed parameter ensemble of HadGEM3-GC3. 05 coupled model projections: part 1: selecting the parameter combinations, Climate Dynamics, 56, 3395-3436, 2021.

Shen, L., Jacob, D. J., Mickley, L. J., Wang, Y., and Zhang, Q.: Insignificant effect of climate change on winter haze pollution in Beijing, Atmospheric Chemistry and Physics, 18, 17489-17496, 10.5194/acp-18-17489-2018, 2018.

Sun, Y., Jiang, Q., Wang, Z., Fu, P., Li, J., Yang, T., and Yin, Y.: Investigation of the sources and evolution processes of severe haze pollution in Beijing in January 2013, Journal of Geophysical Research: Atmospheres, 119, 4380-4398, 2014.

Tie, X., Huang, R.-J., Cao, J., Zhang, Q., Cheng, Y., Su, H., Chang, D., Pöschl, U., Hoffmann, T., and Dusek, U.: Severe pollution in China amplified by atmospheric moisture, Scientific Reports, 7, 1-8, 2017.

Wang, J.-L., Zhang, Y.-h., Shao, M., Liu, X.-l., Zeng, L.-m., Cheng, C.-l., and Xu, X.-f.: Quantitative relationship between visibility and mass concentration of PM2. 5 in Beijing, Journal of environmental sciences, 18, 475-481, 2006.

Wang, L., Wei, Z., Yang, J., Zhang, Y., Zhang, F., Su, J., Meng, C., and Zhang, Q.: The 2013 severe haze over southern Hebei, China: model evaluation, source apportionment, and policy implications, Atmospheric Chemistry and Physics, 14, 3151-3173, 2014a.

Wang, Y., Yao, L., Wang, L., Liu, Z., Ji, D., Tang, G., Zhang, J., Sun, Y., Hu, B., and Xin, J.: Mechanism for the formation of the January 2013 heavy haze pollution episode over central and eastern China, Science China Earth Sciences, 57, 14-25, 2014b.

Xu, M., Chang, C. P., Fu, C., Qi, Y., Robock, A., Robinson, D., and Zhang, H. m.: Steady decline of east Asian monsoon winds, 1969–2000: Evidence from direct ground measurements of wind speed, Journal of Geophysical Research: Atmospheres, 111, 2006.

Xu, P., Chen, Y., and Ye, X.: Haze, air pollution, and health in China, Lancet, 382, 2067, 10.1016/S0140-6736(13)62693-8, 2013.

Yamazaki, K., Sexton, D. M., Rostron, J. W., McSweeney, C. F., Murphy, J. M., and Harris, G. R.: A perturbed parameter ensemble of HadGEM3-GC3. 05 coupled model projections: part 2: global performance and future changes, Climate Dynamics, 56, 3437-3471, 2021.

Yin, Z., and Wang, H.: Role of atmospheric circulations in haze pollution in December 2016, Atmospheric Chemistry and Physics, 17, 11673-11681, 10.5194/acp-17-11673-2017, 2017.

Zhang, Q., Ma, Q., Zhao, B., Liu, X., Wang, Y., Jia, B., and Zhang, X.: Winter haze over North China Plain from 2009 to 2016: Influence of emission and meteorology, Environ Pollut, 242, 1308-1318, 10.1016/j.envpol.2018.08.019, 2018.

Zhang, R., Jing, J., Tao, J., Hsu, S.-C., Wang, G., Cao, J., Lee, C. S. L., Zhu, L., Chen, Z., and Zhao, Y.: Chemical characterization and source apportionment of PM 2.5 in Beijing: seasonal perspective, Atmospheric Chemistry and Physics, 13, 7053-7074, 2013.

Zhang, L., Wilcox, L. J., Dunstone, N. J., Paynter, D. J., Hu, S., Bollasina, M., ... & Zou, L. (2021). Future changes in Beijing haze events under different anthropogenic aerosol emission scenarios. Atmospheric Chemistry and Physics, 21(10), 7499-7514.

Zhang, Z., Gong, D., Mao, R., Kim, S. J., Xu, J., Zhao, X., and Ma, Z.: Cause and predictability for the severe haze pollution in downtown Beijing in November-December 2015, Sci Total Environ, 592, 627-638, 10.1016/j.scitotenv.2017.03.009, 2017.